Large-eddy simulation of saltation over a gaussian dune

Jianzhao Wu[a], Catherine Le Ribault[a], Ivana Vinkovic[a], Serge Simoëns[a]

a. LMFA, UMR CNRS 5509, Ecole Centrale de Lyon, Université de Lyon I, INSA Lyon, France

Résumé :

L'objectif de cette étude est de développer une méthode numérique pour simuler des écoulements turbulents sur des terrains complexes. La simulation des grandes échelles (SGE) est utilisée pour calculer l'écoulement du fluide. Cette méthode est couplée avec une méthode de frontière immergée, qui utilise un forçage direct selon une méthode proposée par Lunquist [1]. Les particules solides sont suivies par une approche lagrangienne. Un modèle d'envol est appliqué pour initialiser le mouvement des particules solides tandis que les interactions entre les particules et le sol sont prises en compte par un modèle de rebond. Un cas canonique d'écoulement turbulent sur une colline gaussienne est utilisé pour valider la méthode de frontière immergée couplée avec la SGE. Les caractéristiques de la zone de recirculation ainsi que des profils de vitesse du fluide et de concentration des particules sont presentés. Le bon accord entre les résultats de la simulation et les donnés expérimentales démontre la fiabilité de cette méthode améliorée, qui sera ensuite appliquée pour des cas de simulation d'écoulement turbulent sur une dune déformable.

Abstract :

The aim of this study is to develop a numerical method to simulate the turbulent boundary flow with solid particle movement over a complex terrain. Large-eddy simulation (LES) is used to compute the flow field with an immersed boundary method, which is imposed by direct forcing as suggested by Lunquist [1]. Solid particles are taken into account through a Lagrangian approach. The entrainment model is applied to initialize the particle movement while particle/soil interaction is accounted for by the rebound model. A canonical simulation case of a turbulent boundary layer flow over a Gaussian dune is performed to verify the accuracy of the immersed boundary method coupled with LES. Recirculation region characteristics, fluid velocity profiles as well as particle concentrations at different streamwise positions are presented. Good agreement between experimental data and simulated results demonstrates the ability of the improved solver, which will be applied to the simulation of turbulent boundary layer flow over a deformable sand dune.

Mots clefs : Simulation des grandes échelles, frontières immergées, saltation, colline gaussienne

1 Introduction

The transport of solid particles by turbulent flows is considered as a common topic in different industrial and environmental problems. In particular, it plays an important role in the aeolian sand erosion, which plays a crucial role in regional desertification. When the sand storm happens, the phenomena of large scale transport of sand particles or dusts can be caught from the view of satellite [2, 3]. It is also observed that the topographic structures of sand dune are effected by the local particle behavior, which is related to the small-scale turbulent structure near the boundary. Unfortunately, the physics behind these natural processes has not yet been in-depth studied.

The pioneering work of sand erosion has been carried out in 1941 by Bagnold [4]. Owen followed this research and used the classical approaches to understand the aeolian process under the steady state assumption [5]. In the recent twenty years, several experimental studies and numerical simulations have been carried out to find the fundamental nature or physics of particle motion following the turbulent flow [6, 7, 8, 9]. According to these studies, the sand particle motion mainly consists of three modes : saltation, suspension and creep. The saltation is the major motion mode for the sand particle movement during the process of sand erosion. Different models has been developed to estimate the interaction of the particles with the soil, such as the aerodynamic entrainment, the rebound and the splash function [4, 10, 11, 12].

In our team, numerical methods have already been developed to simulate the saltation and the transport of solid particles in boundary layers [13]. The fluid flow is taken into account through large eddy simulations (LES) using the Advanced Regional Prediction System (ARPS) code [14]. This approach allows the computation of the instantaneous evolution of large turbulent structures able to produce sweeping events responsible for aerodynamic entrainment of solid particles. To take into account the solid particles, a Lagrangian tracking model is coupled with the LES. Different models have been introduced to take into account the interactions of the particles with the soil, especially the aerodynamic entrainment and the rebound. The numerical method has been used to study the TBL flow with or without solid particles over one hill or several successive hills, and the simulated results were compared with the experimental results by Simoëns *et al.* [9]. However, the LES approach, based on finite differences on structured grids, is not able to simulate moving or deformable complex terrains. Therefore, the first goal of our present work is to modify the numerical approach to simulate turbulent flow on a moving and deformed surface. An immersed boundary method (IBM) proposed by Lunquist [1], has been introduced in ARPS to enable the LES with moving or deformable terrain. It is a direct forcing approach and the boundary conditions are directly imposed on the immersed surface. Due to the use of a simple Cartesian mesh, the immersed boundary method avoids the mesh regeneration process after the boundary deforms or moves, and therefore reduces the computing cost and time [1, 16].

The purpose of this paper is to develop a new numerical method for LES coupled with IBM, which will be applied to the simulation of deformation of sand dunes. In sections 2 and 3, we present fluid and particle governing equations, the numerical method, as well as the physical model for sand grain and bed interaction. The experimental set-up used for validation is briefly presented in section 4. Finally, the first validation on the canonical case of a turbulent boundary flow over a Gaussian hill is illustrated.

2 Fluid phase

The motion of the fluid phase is governed by the simplified Navier-Stokes equations under the Boussinesq approximation. Numerical simulations are performed by the LES approach coupled with the immersed boundary method. The numerical method has been implemented in the ARPS code.

2.1 Governing equation

When the actual pressure, density and potential temperature are close to a hydrostatic state, which is defined as the base state by setting null velocity distribution, a simplification of Navier-Stokes equations is carried out by taking into account their variations. In ARPS, the simplified governing equations of fluid velocity, variation of pressure, density and temperature using the Boussinesq approximation are given by

$$\frac{\partial(\Delta p)}{\partial t} + u_i \frac{\partial(\Delta p)}{\partial x_i} = \rho_r g u_i \delta_{i3} - \rho_r c_s^2 \frac{\partial u_i}{\partial x_i}, \tag{1}$$

$$\frac{\partial(\Delta \theta)}{\partial t} + u_i \frac{\partial(\Delta \theta)}{\partial x_i} = -u_i \frac{\partial \theta_r}{\partial x_i} + k_T \frac{\partial^2 \theta}{\partial x_i \partial x_i}, \tag{2}$$

$$\frac{\partial u_i}{\partial t} + u_j \frac{\partial u_i}{\partial x_j} = -\frac{1}{\rho_r} \frac{\partial(\Delta p)}{\partial x_i} - g\delta_{i3} \left(\frac{\Delta \theta}{\theta_r} - \frac{\Delta p}{\rho_r c_s^2} \right) - 2\epsilon_{ijk}\Omega_j u_k + \frac{1}{\rho_r} \frac{\partial \pi_{ji}}{\partial x_j}, \tag{3}$$

where Δ denotes the variation to the base state, the subscript r means the base state, $x_i = (x, y, z)$ the position, $u_i = (u, v, w)$ the fluid velocity, ρ the fluid density, p the pressure, θ the potential temperature, g the gravity, Ω_j the angular velocity of the earth's rotation, δ_{ij} the Kronecker tensor, ϵ_{ijk} the Levi-Civita symbol, $\pi_{ij} = \mu(\partial u_i/\partial x_j + \partial u_j/\partial x_i - 2/3\delta_{ij}\partial u_j/\partial x_j)$ the stress tensor, μ the fluid dynamic viscosity and k_T the heat mixing coefficient, respectively. Eq. (1) is the combination of the continuity equation and the equation of state. Eq. (2) indicates the temporal evolution of potential temperature perturbation. Finally Eq. (3) is the simplified momentum equation. The adiabatic term in the pressure variation equation has be eliminated because the divergence term is usually dominant.

2.2 Large-eddy simulation

In the Large-eddy simulation, a truncation at low wave numbers is applied in order to obtain the large scale component. After the low-pass (grid scale) filter is applied to the fluid velocity and taking advantage of the quasi-incompressible hypothesis $\partial u_i/\partial x_i \approx 0$, Eq. (3) becomes

$$\frac{\partial u_i^<}{\partial t} + u_j^< \frac{\partial u_i^<}{\partial x_j} = -\frac{1}{\rho_r} \frac{\partial(\Delta p)}{\partial x_i} - g\delta_{i3} \left(\frac{\Delta \theta}{\theta_r} - \frac{\Delta p}{\rho_r c_s^2} \right) - 2\epsilon_{ijk}\Omega_j u_k^< + \frac{1}{\rho_r} \frac{\partial \pi_{ji}^<}{\partial x_j} + \frac{\partial \tau_{ji}^<}{\partial x_j}, \tag{4}$$

in which the subgrid stress is defined as

$$\tau_{ij}^< = (u_i u_j)^< - u_i^< u_j^<. \tag{5}$$

Generally, the subgrid stress can also be modeled by a subgrid viscosity ν_{sgs} as

$$\tau_{ij}^< = \nu_{sgs} \left(\frac{\partial u_i^<}{\partial x_j} + \frac{\partial u_j^<}{\partial x_i} - \frac{2}{3} \frac{\partial u_j^<}{\partial x_j} \delta_{ij} \right). \tag{6}$$

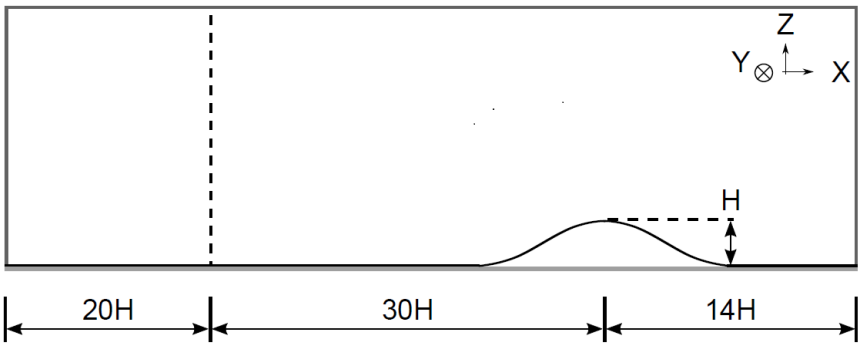

FIGURE 1 – Sketch of the computational domain.

In ARPS, the subgrid viscosity ν_{sgs} is assumed to be a function of the turbulent kinetic energy k_{sgs} and the mixing length l_m :

$$\nu_{sgs} = C_s l_m \sqrt{k_{sgs}}, \tag{7}$$

with the constant coefficient C_s, which takes the value of 0.1 according to Moeng & Wyngaard [17]. k_{sgs} is calculated by an additional turbulent kinetic energy transport equation, which is detailed more precisely in these literatures [18, 19]. The mixing length is generally assigned by the grid size, which can be represented as the smallest resolved scale. It should be noted that the temperature flux obtained after the filter is applied to Eq. (2), has also been approximated by the sub-grid scale (SGS) model.

2.3 Numerical parameters

In our simulations, the inlet condition is generated by an approach proposed by Lund *et al.* [20]. Fluctuations are extracted from a downstream station, rescaled to take into account the development of the boundary layer and reinjected at the inlet station. The radiative condition is employed at the outlet station, the zero-normal gradient condition is set at the top boundary, and the free-slip condition is applied to the bottom surface of the computing domain. The Gaussian dune on the lower wall is modeled by an immersed boundary method which is described in the following paragraph.

The computational domain is illustrated in Fig.1. The Gaussian hill is located at $x = 50H$, where H is the height of the hill. At the beginning of the domain, there is a development section from $x = 0$ to $x = 20H$ for generating the inlet flow. The physical parameters and the numerical parameters are shown in detail in Tab. 1. The external velocity U_∞, the boundary layer thickness δ and the friction velocity u_* are given to generate the inlet streamwise velocity profile and the initial base state through an improved log-law formula [15, 21]. The size of the domain is determined by L_x, L_y and L_z and N_x, N_y and N_z are the number of nodes in the three direction. The grid is uniform in the streamwise and spanwise direction with the assigned values Δx and Δy. It is slightly stretched in the wall-normal direction with a refined increment near the wall Δz_{min}.

$H(m)$	$\delta(m)$	$U_\infty(m/s)$	$u_*(m/s)$	δ^+	Δz^+_{min}	$Re = HU_\infty/\nu$
0.01	0.07	11.2	0.46	2147	15	7467
$N_x \times N_y \times N_z$	L_x/H	L_y/H	L_z/H	$\Delta x/H$	$\Delta y/H$	$\Delta z_{min}/H$
$643 \times 63 \times 100$	64	6	15	0.1	0.1	0.05

TABLE 1 – Physical parameters and numerical parameters.

2.4 Immersed boundary method

The immersed boundary approach allows us to use a Cartesian grid to simulate a turbulent boundary layer flow over a complex surface. The new boundary condition is implicitly applied by adding a forcing term f_i to the momentum equation Eq. (3), leading to

$$\frac{\partial u_i}{\partial t} = -u_j \frac{\partial u_i}{\partial x_j} - \frac{1}{\rho_r}\frac{\partial(\Delta p)}{\partial x_i} - g\delta_{i3}\left(\frac{\Delta\theta}{\theta_r} - \frac{\Delta p}{\rho_r c_s^2}\right) - 2\epsilon_{ijk}\Omega_j u_k + \frac{1}{\rho_r}\frac{\partial \pi_{ji}}{\partial x_j} + f_i \tag{8}$$

A simple discrete form of Eq.(8) is used considering an explicit scheme

$$\frac{u_i^{n+1} - u_i^n}{\Delta t} = RHS_i^n + f_i^n, \tag{9}$$

where n is the present time step, RHS_i^n denotes the sum of all discrete terms at the right hand side of Eq. (8), except for f_i. If we consider a boundary with a velocity U_i^d , then the no-slip condition leads to the following expression for f_i^n

$$f_i^n = \frac{U_i^d - u_i^n}{\Delta t} - RHS_i^n. \tag{10}$$

Generally, the forcing is not applied on the real boundary. It is constrained on chosen ghost cells, where the prescribed velocity U_i^d is obtained by an interpolation scheme. In our simulation, the prescribed velocity is given through the interpolation between the image point of ghost cells and its neighboring fluid cells, as proposed by Lundquist [1].

3 Solid phase

The solid phase is described by the Lagrangian tracking of small, pointwise, solid particle at low volume fraction. A take off model is introduced for the particle entrainment as well as a rebound model for the interaction between solid particles and the surface. The governing equations as well as the modeling approach are described in the following paragraphs.

3.1 Governing equation

Pointwise, solid particles with a diameter smaller than the Kolmogorov scale are considered here. At low volume fractions and high density ratios between the solid phase and the fluid, the only forces that are taken into account are the aerodynamic drag force and the gravity. This leads to the following set of equations :

$$\begin{aligned} \frac{dx_i^p}{dt} &= v_i^p, \\ \frac{dv_i^p}{dt} &= \frac{u_i(x_i^p(t), t) - v_i^p(t)}{\tau^p} + g\delta_{i3}, \end{aligned} \tag{11}$$

where the sign $(\cdot)^p$ denotes quantities related to the solid particle, x_i^p is the particle position, v_i^p the particle velocity, $u_i(x_i^p(t), t)$ the fluid velocity at the particle position, τ^p the particle relaxation time, g the gravity acceleration, respectively. In fact, τ^p represents the characteristic time scale of the particle motion relative to the turbulent flow, and takes the form of

$$\tau^p = \frac{\rho^p d^{p2}}{18\rho\nu} f(Re^p)^{-1}, \tag{12}$$

with $Re^p = |u - v^p| d^p / \nu$ denoting the particle Reynolds number, ρ^p the sand density and d^p the diameter of sand grain. The function f is given by

$$f(Re^p) = \begin{cases} 1 + 0.15 Re^{p0.687}, & \text{if } Re^p < 1000; \\ 0.0183 Re^p, & \text{otherwise.} \end{cases} \tag{13}$$

It should be noted that the relaxation time takes the simplest form $\tau_c^p = \dfrac{\rho^p d^{p2}}{18\rho\nu}$ if the particle Reynolds number is small $Re^p \ll 1$, which is widely used in literatures [13, 22].

The Stokes number is defined as the ratio of τ_c^p and the characteristic time scale of fluid. Using the turbulent integral time scale $T_L = \delta / u_*$, we have

$$St_L = \frac{\tau_c^p}{T_L}, \tag{14}$$

alternatively, using the Kolmogorov time scale $T_\eta = \sqrt{\nu\delta / u_*^3}$, we obtain

$$St_\eta = \frac{\tau_c^p}{T_\eta}, \tag{15}$$

In our simulation, the detailed information of parameters of solid phase is presented in Tab. 2. The Shields number $Sh = \dfrac{\rho u_*^2}{(\rho^p - \rho) g d^p} = 0.14$ reveals that saltation and suspension are two main modes of the particle motion ; As the particle relaxation time scale τ_c^p satisfies $T_\eta \ll \tau_c^p < T_L$, the particle motion is hardly responsive to the turbulent dissipative scale structure, but can be easily influenced by the energetic scale structure.

$\rho^p (kg/m^3)$	$d^p (\mu m)$	$g (m^2/s)$	$\tau_c^p (s)$	Sh	St_L	St_η
1000	200	9.81	0.12	0.14	0.75	35.01

TABLE 2 – Parameters of solid phase.

3.2 Take off model

A take off model is used for aerodynamic entrainment of solid particles. Based on the balance of forces acting on a particle, Bagnold [4] has established the first formula of the threshold friction velocity by only considering the aerodynamic drag and gravity, and then Greeley [10] and Shao [11] improved Bagnold's model by introducing the adhesion force acting between particles. In general, the average friction velocity is used to verify the criterion. In our work, the take off model is improved by considering the instantaneous forces as proposed by Huang [15]. Based on the balance of the gravity force P, the adhesion force F_A, and the lift force F_L, the new criterion is established as

$$F_L \geq P + F_A. \tag{16}$$

In fact, the gravity is given by $P = \dfrac{1}{6}(\rho^p - \rho) g d^{p3}$, and the adhesion force is evaluated as $F_A = c_0 d^p$ with the coefficient $c_0 = 1.43 \times 10^{-5} N \cdot m^{-1}$. According to the experimental results of Mollinger and

Niewstadt [23], the mean lift force can be expressed by

$$\overline{F_L} = 1.55\rho\nu^2 \left(\frac{d^p \sqrt{\tau_w/\rho}}{\nu} \right)^{1.87}. \tag{17}$$

Based on the quadrant analysis, the stress near the wall $\tau_w = \langle u'w' \rangle$ can be divided into four parts : the outward interaction $\tau_w^1 = \langle u'_\oplus w'_\oplus \rangle$, the ejection $\tau_w^2 = \langle u'_\ominus w'_\oplus \rangle$, the inward interaction $\tau_w^3 = \langle u'_\ominus w'_\ominus \rangle$ and the sweep $\tau_w^4 = \langle u'_\oplus w'_\ominus \rangle$, where $u'_\oplus$ ($u'_\ominus$), $w'_\oplus$ ($w'_\ominus$) is assigned by u', w', respectively. It is observed that the sweep term τ_w^4 not only is one of the dominant term of the wall stress, but also plays a crucial role in the process of particle transport. Therefore, the instantaneous lift force is evaluated by

$$F_L = \frac{u'_\oplus w'_\ominus}{\langle u'_\oplus w'_\ominus \rangle} \overline{F_L}. \tag{18}$$

3.3 Rebound model

Due to the effect of gravity, particles fall and impact the surface with large momentum. Particles that reach the ground may be deposited or they can rebound and continue their movement within the fluid phase. As the collision time scale is smaller than the turbulent small time scale, the rebound process is modeled independently of the fluid motion. Generally, particle motion after rebound can be described by the rebound angle and the norm of its new velocity. In our study, the model proposed by Beladjine *et al.* [12] is used. In this model, the angle θ_r and the velocity norm V_r for a two-dimensional case follow a Gaussian distribution and their mean values are given according to :

$$\begin{aligned} \overline{\theta_r} &= \arcsin\left(\frac{A_z - B_z \sin\theta_i}{A - B\sin\theta_i} \right) + \alpha_0, \\ \overline{V_r} &= (A - B\sin\theta_i) V_i \end{aligned} \tag{19}$$

where $A_z = 0.30$, $B_z = 0.15$, $A = 0.87$, and $B = 0.72$, V_i is the incident velocity norm, θ_i is the incident angle, the angle α_0 is the local slope. Their standard deviation is assumed as $\sigma_{\theta_r} = \overline{\theta_r}$ and $\sigma_{V_r} = (2 - \theta_r/\overline{\theta_r})\overline{V_r}$. When this model is applied to a three-dimensional case, the horizontal rebound angle φ_r is taken into account and is assumed as a random parameter following a Gaussian distribution with the zero mean and a standard deviation of $10°$. Therefore, the new velocity norm is given by $V_r/\cos\varphi_r$.

4 Experimental set-up

The experiment of the turbulent boundary layer flow over a Gaussian hill has been carried out by Simoëns *et al.* [9]. The height of the sand dune with maximal slope $31°$ is $H = 0.01\ m$, and the external velocity is set to $U_\infty = 11.2\ m/s$. Sand particles with a density of $1000\ kg/m^3$ are placed in a box $20\ cm \times 10\ cm$ located at the beginning of the fluid domain. The particle diameter has a mean value of $200\ \mu m$ and ranges from $170\ \mu m$ to $250\ \mu m$. These particles are lifted off by the flow. The fluid velocity is measured by particle image velocimetry (PIV). The sand particle concentration and velocity are calculated by digital image treatment.

5 Validation : flow over a Gaussian hill

The first verification has been carried out on the simulation of a turbulent boundary layer flow over a Gaussian hill. Two numerical simulation cases are provided to analyze :

— LES case : simulated by the ARPS using the body-conformal grid without imposing the immersed boundary condition.

— LES&IBM case : simulated by the ARPS coupled with the immersed boundary method using the Cartesian grid.

With regard to the fluid field, we study the characteristic of the recirculation zone and present the profile of the mean longitudinal velocity and of the Reynold stress. For the solid phase, particle trajectories are presented as well as particle concentration and streamwise velocity profiles. Comparison with the results simulated by ARPS and the experimental data is provided.

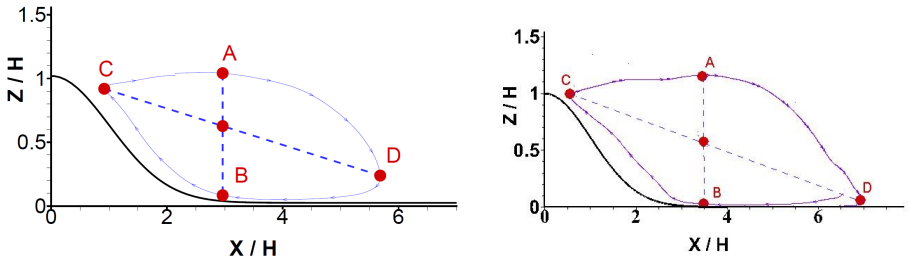

FIGURE 2 – Recirculation zone on the lee side of the Gaussian hill. Left : ARPS simulation (LES), $L_{AB} = 0.96H$, $L_{CD} = 4.81H$, $L_{AB}/L_{CD} = 0.20$. Right : ARPS simulation coupled with the immersed boundary method (LES&IBM), $L_{AB} = 1.01H$, $L_{CD} = 6.33H$, $L_{AB}/L_{CD} = 0.16$.

5.1 Fluid

The fluid field is of primary importance for our simulation. Firstly, the recirculation zone on the lee side of the Gaussian dune is illustrated in Fig. 2. The shape of the recirculation zone can be defined by two following parameters : a major segment L_{CD} and a minor one L_{AB} (as illustrated in Fig.2). Figure 1 shows the recirculation zone obtained by ARPS and by the LES coupled with the immersed boundary method. The length L_{AB} is roughly the same between the two sets of simulations, whereas L_{CD} is greater when the immersed boundary method is introduced. This means that the recirculation zone size obtained by coupling ARPS with an immersed boundary method is slightly larger than the one obtained by the standard ARPS model, but the new size is consistent with the experimental results ($L_{AB} = 1.2$, $L_{CD} = 6.7$) of Simoëns *et al.* [9].

The normalized mean longitudinal velocity over a Gaussian is presented in Fig. 3. It is shown that the flow near the boundary accelerates on the windward side of the dune and then decreases on its lee side. The velocity profiles located in the recirculation zone are reversed. The good agreement between the simulation results and experimental data shows the rationality and accuracy of the new LES approach coupled with the immersed boundary method.

In Fig. 4, we illustrate profiles of mean Reynolds stress, which is important for the particle aerodynamic entrainment. Because of the separation of shear flow, the Reynold stress increases obviously in the recirculation zone. The Reynolds stress simulated is smaller than that of experiments. Globally, the agreement on Reynolds stress, particularly near the wall, ensures us the validity of the new method.

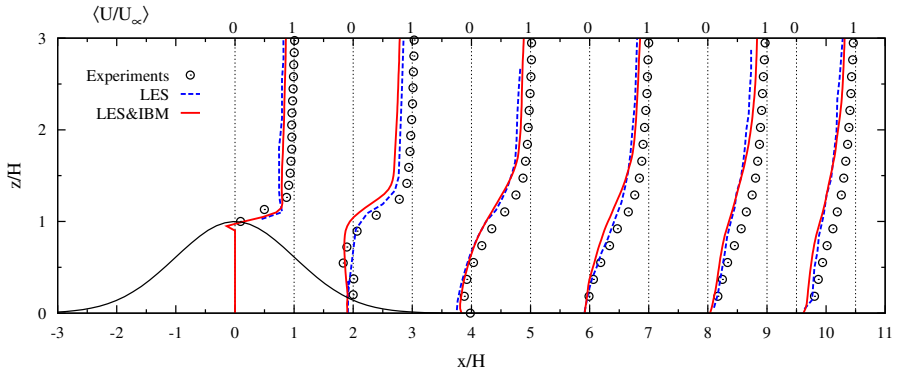

FIGURE 3 – Mean longitudinal velocity profiles over a Gaussian hill. Points : experiments of Simoëns *et al.* [9]. Dashed lines : ARPS simulation (LES). Solid lines : ARPS simulation coupled with the immersed boundary method (LES&IBM).

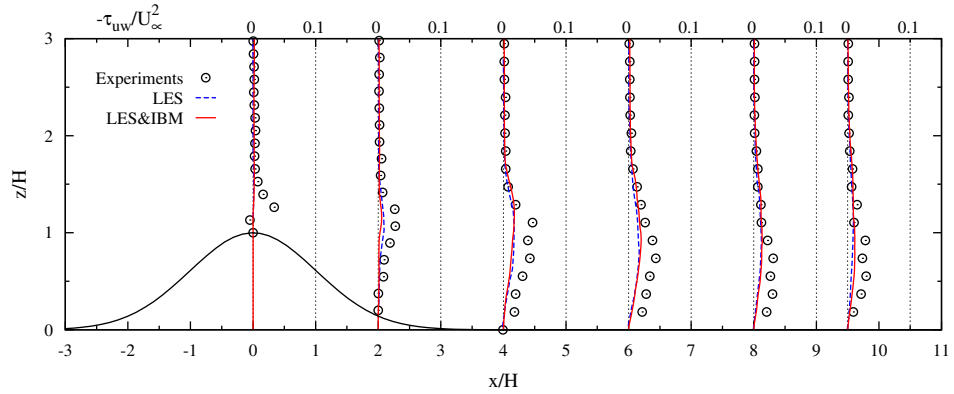

FIGURE 4 – Reynold stress $\tau_{uw} = \langle u'w' \rangle$ profiles over a Gaussian hill. Points : experiments of Simoëns [9]. Dashed lines : ARPS simulation (LES). Solid lines : ARPS simulation coupled with the immersed boundary method (LES&IBM).

5.2 Particle transport

Fig.5 shows several sand particle trajectories around the Gaussian hill. Sand particles are aerodynamically entrained at the location of the sand box. Once lifted-off, particles are transported by the fluid. By the action of gravity they might impact the wall and rebound. According to the rebound model proposed by Beladjine *et al.* [12], particles that impact the hill on the upstream side are highly dispersed in the flow.

The profiles of particle concentration over a fixed Gaussian dune are shown in Fig.6. Each profile is normalized by its maximal concentration. High values of the concentration are obtained close to the surface and in the mixing layer at the interface of the recirculation region and the outer flow. Behind the hill, in the recirculation region, particle concentration is low and drops to zero. Globally, very good agreement is obtained between simulation results and experimental data. The locations of the concentration peak are well predicted by both simulations (LES and LES&IBM).

The comparison between the particle and fluid longitudinal velocity is shown on Fig.7. The velocity is normalized by U_∞. Due to the presence of zero concentration, an apparent discontinuity exists on the particle velocity profile after the dune. On the upstream side, the fluid and particle velocities are close.

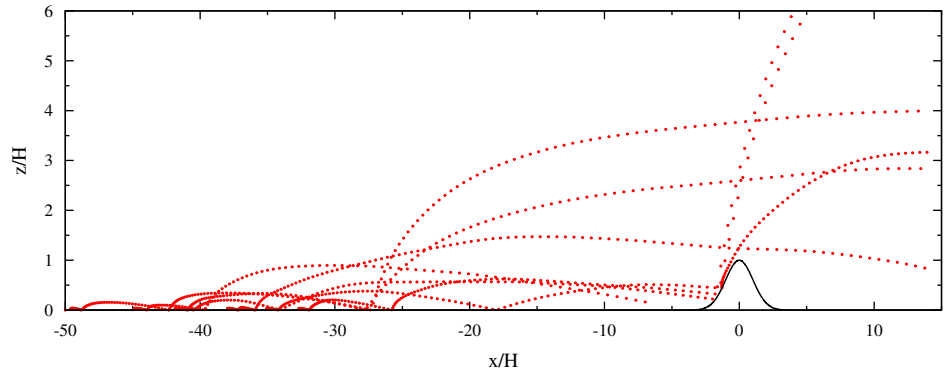

FIGURE 5 – Particle trajectories over a Gaussian hill.

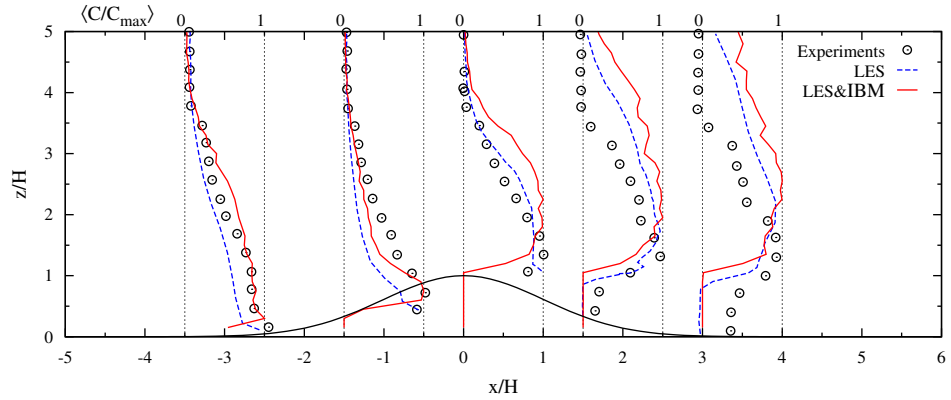

FIGURE 6 – Particle concentration profiles over a Gaussian hill. Points : experiments of Simoëns *et al.* [9]. Dashed lines : ARPS simulation (LES). Solid lines : ARPS simulation coupled with the immersed boundary method (LES&IBM).

Over the dune, the particle velocity is obviously smaller than the fluid. Due to the presence of the dune, the fluid velocity increases more rapidly than the particle's because of the particle response time to fluid solicitations (τ^p).

6 Conclusions and perspectives

In this study, a large-eddy simulation is coupled with immersed boundary method to simulate turbulent boundary layer flow over a Gaussian hill with Lagrangian tracking of solid particles. The first validation has been carried out on a turbulent boundary layer flow over a Gaussian hill. The accuracy and effectiveness of this method is demonstrated by the good agreement between the (LES and LES&IBM) simulation results and experimental data. In our future work, this approach will be used to simulate the turbulent boundary layer flow with a deformable and moving dune. The deformation of the dune will be modeled by sand particle movement with those particle/soil models proposed by Lopes [24].

Références

[1] K. A. Lundquist, F. K. Chow, J. K. Lundquist, An immersed boundary method for the weather research and forecasting model, Monthly Weather Review, 138.3 (2010) 796–817.

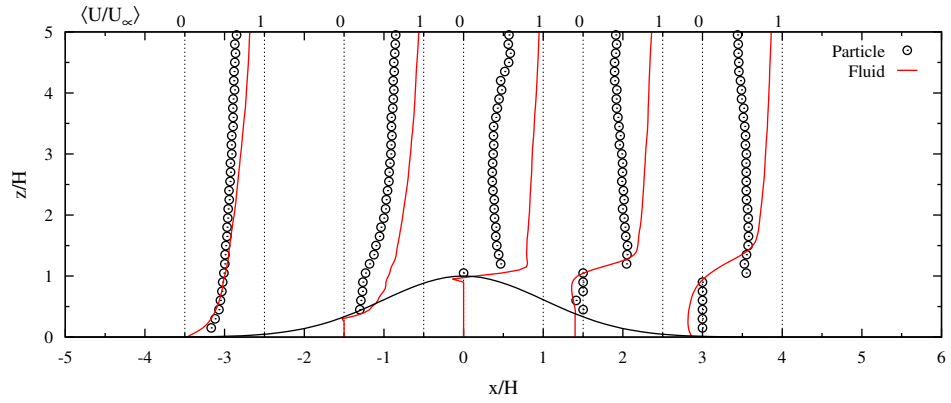

FIGURE 7 – Comparison between particle longitudinal velocity (points) and fluid velocity (lines) over a Gaussian hill. Results obtained by ARPS simulation coupled with the immersed boundary method (LES&IBM).

[2] X. Zheng, Mechanics of wind-blown sand movements, Springer Science & Business Media, 2009.

[3] Y. Shao. Physics and modeling of wind erosion, Vol. 37, Springer Science & Business Media, 2008.

[4] R.A. Bagnold, The physics of wind blown sand and desert dunes, London, 1941.

[5] P.R. Owen, Saltation of uniform grains in air, Journal of Fluid Mechanics, 20.02 (1964) 225–242.

[6] R.S. Anderson, M. Sϕrensen, and B. B. Willetts, A review of recent progress in our understanding of aeolian sediment transport, Aeolian Grain Transport 1, Springer Vienna, (1991)1–19.

[7] Y. Shao, and A. Li, Numerical modeling of saltation in the atmospheric surface layer, Boundary-Layer Meteorology, 91.2 (1999) 199–225.

[8] T.D. Ho, A. Valance, P. Dupont. A.O. El Moctar, Aeolian sand transport : Length and height distributions of saltation trajectories, Aeolian Research, 12 (2014) 65–74.

[9] S. Simoëns, S. Saleh, C. Le Ribault, M. Belmadi, R. Zegadi, F. Allag, J.M. Vignon, G. Huang, Influence of Gaussian hill on concentration of solid particles in suspension inside turbulent boundary layer, Procedia IUTAM, 17 (2015) 110-118.

[10] R. Greeley, J.D. Iversen, Wind as a geological process : on Earth, Mars, Venus and Titan, Cambridge University Press, New York, 1985.

[11] Y. Shao, H. Lu, A simple expression for wind erosion threshold friction velocity, Journal of Geophysical Research : Atmospheres, 105.D17(2000) 22437–22443.

[12] D. Beladjine, M. Ammi, L. Oger, A. Valance, Collision process between an incident bead and a three-dimensional granular packing, Physical Review E, 75.6(2007) 061–305.

[13] I. Vinkovic, C. Aguirre, M. Ayrault, S. Simoëns, (2006). Large-eddy simulation of the dispersion of solid particles in a turbulent boundary layer, Boundary-Layer Meteorology, 121 (2006) 283-311.

[14] M. Xue, K. K. Droegemeier, V. Wong, The Advanced Regional Prediction System (ARPS) - A multi-scale non-hydrostatic atmospheric simulation and prediction model. Part I : Model dynamics and verification, Meteorology and atmospheric physics, 75.3 (2000) 161–193.

[15] G. Huang, Numerical simulation of solid particle transport in atmospheric boundary-layer over obstacles, Thèse, Ecole Centrale de Lyon, 2016.

[16] R. Mittal, G. Iaccarino, Immersed boundary methods, Annu. Rev. Fluid Mech., 37 (2005) 239–261.

[17] C. H. Moeng, J. C. Wyngaard, Evaluation of turbulent transport and dissipation closures in second-order modeling, Journal of the Atmospheric Sciences, 46.14 (1989) 2311-2330.

[18] J. W. Deardorff, Stratocumulus-capped mixed layers derived from a three-dimensional model, Boundary-Layer Meteorology, 18.4 (1980) 495-527.

[19] C. H. Moeng, A large-eddy-simulation model for the study of planetary boundary-layer turbulence, Journal of the Atmospheric Sciences, 41.13 (1984) 2052-2062.

[20] T. S. Lund, X. Wu, K. D. Squires, Generation of turbulent inflow data for spatially-developing boundary layer simulations, Journal of Computational Physics, 140.2 (1998) 233-258.

[21] G. Huang, S. Simoëns, I. Vinkovic, C. Le Ribault, S. Dupont, G. Bergametti, Law-of-the-wall in a boundary-layer over regularly distributed roughness elements, Journal of Turbulence, 17.5 (2016) 518-541.

[22] S. Dupont, G. Bergametti, B. Marticorena, S. Simoëns, Modeling saltation intermittency. Journal of Geophysical Research : Atmospheres, 118.13 (2013) 7109-7128.

[23] A. M. Mollinger, F. T. M. Nieuwstadt, Measurement of the lift force on a particle fixed to the wall in the viscous sublayer of a fully developed turbulent boundary layer, Journal of Fluid Mechanics, 316 (1996) 285-306.

[24] A. M. G. Lopes, L. A. Oliveira, A. D. Ferreira, J. P. Pinto, Numerical simulation of sand dune erosion, Environmental fluid mechanics, 13.2 (2013) 145-168.